presence of two different metal centers, which manifests itself most prominently in the metal–hydride bonding, a result of the greater strength of Ir–H vs Rh–H bonds. Although species with close-to-symmetric Rh–H–Ir bridges have been observed, in several complexes relatively weak Rh–H interactions appear to be present as evidenced by the smaller NMR couplings between rhodium and hydride ligand as well as between the hydride and rhodium-bound phosphorus nuclei. It is also significant that the cationic species **3** differs appreciably from the Rh₂ and Ir₂ analogues in that it has no bridging carbonyl group. Clearly the mixed-metal complexes will not always have properties intermediate between those of the homobimetallic analogues but will show some unique characteristics by virtue of the polarity induced in a heterobinuclear system. These are the first mixed-metal rhodium–iridium complexes prepared that contain only carbonyl and hydride ligands besides the bridging diphosphines. The interconversions via simple

hydrogenation, carbonylation, protonation, and deprotonation steps illustrate their potential utility for modeling catalytic processes, studies of which are presently underway in this group.

Contribution from the School of Chemistry, University of New South Wales,
P.O. Box 1, Kensington, NSW 2033, Australia

A New Three-Dimensionally Nonmolecular Cd–S Lattice in Crystalline Cd₇(SC₆H₄CH₃-2)₁₄(DMF)₂

Ian G. Dance,* Robert G. Garbutt, and Marcia L. Scudder

Bis(2-methylbenzenethiolato)cadmium crystallizes from DMF as Cd₇(SC₆H₄CH₃-2)₁₄(DMF)₂ (**5**) and has a three-dimensionally nonmolecular crystal structure quite different from those of Cd(SC₆H₅)₂ and 4-substituted Cd(SC₆H₄X)₂. The crystals (tetragonal, $P4_32_12$, $a = b = 14.028$ (1) Å, $c = 55.295$ (8) Å, $V = 10\,880.7$ (1.9) Å³, $Z = 8$ (× Cd₃.₅S₇C₄₉H₄₉·C₃H₇NO), 4311 independent observed ($I/\sigma(I) > 3$) data (Mo Kα), $R = 0.034$) contain {Cd₃(μ-SAr)₃(DMF)} cycles, in which the DMF carbonyl oxygen atom has asymmetric secondary coordination (Cd–O = 2.72, 2.95, 2.99 Å) to the three Cd atoms with tetrahedral Cd(μ-SAr)₄/₂ primary coordination. The Cd₃ cycles are linked by (μ-SAr) ligands and spiro Cd atoms. The unique structural feature of these three-dimensionally nonmolecular linkages is the occurrence of large open elongated macrocycles, ca. 28 Å long and 14 Å wide, around which the pathway with the smallest number of connections involves 24 Cd atoms and 24 bridging thiolate ligands. Adamantanoid cages are absent.

Introduction

We are investigating the structures and reactions of the class of compounds Cd(SR)₂ and recently reported the crystal structures of the aryl derivatives Cd(SPh)₂ (**1**), Cd(SC₆H₄F-4)₂ (**2**), Cd(SC₆H₄CH₃-4)₂ (**3**), and Cd₈(SC₆H₄Br-4)₁₆(DMF)₃ (**4**), all crystallized from DMF.[1-3] Crystalline **1–3** are three-dimensionally nonmolecular. They comprise adamantanoid cages, each with an {*octahedro*-(μ-SAr)₆-*tetrahedro*-Cd₄} core and with four intercage linkages through shared SAr ligands at the vertices of the tetrahedral adamantanoid units: the general formula is thus $^3_\infty[(\mu\text{-SAr})_6Cd_4(\mu\text{-SAr})_{4/2}]$.

Alternatively, these structures can be considered as three-dimensional Cd–S lattices, adorned with substituents. In this view, the Cd(SAr)₂ structures are comparable with the lattices of silicates, aluminosilicates, and aluminophosphates.[4] The topological correspondence is between the tetrahedral adamantanoid cage [(μ-SAr)₆Cd₄(μ-SAr)₄/₂] and the tetrahedral TO₄ unit (T = Al, Si, P), which is much smaller. Indeed, the lattice adopted by **1** and **2** is isostructural with that of α-cristobalite, and **3** is analogous to a zeolite with cavities and channels, but with much larger dimensions. The stoichiometries of the metal sulfide lattice in Cd(SAr)₂ compounds and of the metal oxide lattices are the same, namely MX₂ (X = O, S). Further, just as the microporous oxide

lattices have spatially differentiated regions of MO₂ framework and of cavity and/or channel, so there is in crystalline **1–3** clear spatial segregation of the CdS₂ framework and the regions occupied only by Ar substituents. The volumes occupied by the Ar substituents are larger, both in actuality and as a proportion of the lattice volume, than the void volumes of the microporous oxides. There is a nice complementarity between these *nonmolecular* Cd–S lattices with internal Ar substituents and *molecular* CdS clusters coated with Ar substituents, such as [S₄Cd₁₀(SPh)₁₆]⁴⁻,[5] [S₄Cd₁₇(SPh)₂₈]²⁻,[6] and stabilized colloidal CdS.[7-10]

(1) Craig, D.; Dance, I. G.; Garbutt, R. *Angew. Chem., Int. Ed. Engl.* **1986**, *25*, 165.

(2) Dance, I. G.; Garbutt, R. G.; Craig, D. C.; Scudder, M. L.; Bailey, T. D. *J. Chem. Soc., Chem. Commun.* **1987**, 1164.

(3) Dance, I. G.; Garbutt, R. G.; Craig, D. C.; Scudder, M. L. *Inorg. Chem.* **1987**, *26*, 4057.

(4) Smith, J. V. *Chem. Rev.* **1988**, *88*, 149–182.

(5) Dance, I. G.; Choy, A.; Scudder, M. L. *J. Am. Chem. Soc.* **1984**, *106*, 6285.

(6) Lee, G. S. H.; Craig, D. C.; Ma, I.; Scudder, M. L.; Bailey, T. D.; Dance, I. G. *J. Am. Chem. Soc.* **1988**, *110*, 4863.

(7) (a) Henglein, A. In *Modern Trends of Colloid Science in Chemistry and Biology*; Eicke, H.-F., Ed.; Birkhaeuser Verlag; Basel, Switzerland, 1985; pp 126–147. (b) Brus, L. *J. Phys. Chem.* **1986**, *90*, 2555–2560. (c) Lianos, P.; Thomas, J. K. *Chem. Phys. Lett.* **1986**, *125*, 299–302. (d) Henglein, A. *Top. Curr. Chem.* **1988**, *143*, 113–175. (e) Spanhel, L.; Hasse, M.; Weller, H.; Henglein, A. *J. Am. Chem. Soc.* **1987**, *109*, 5649–5655.

(8) (a) Youn, H.-C.; Baral, S.; Fendler, J. H. *J. Phys. Chem.* **1988**, *92*, 6320–7. (b) Zhao, X. K.; Baral, S.; Rolandi, R.; Fendler, J. H. *J. Am. Chem. Soc.* **1988**, *110*, 1012–1024. (c) Baral, S.; Fendler, J. H. *J. Am. Chem. Soc.* **1989**, *111*, 1604.

(9) (a) Thayer, A. M.; Steigerwald, M. L.; Duncan, T. M.; Douglass, D. C. *Phys. Rev. Lett.* **1988**, *60*, 2673–2676. (b) Steigerwald, M. L.; Alivisatos, A. P.; Gibson, J. M.; Harris, T. D.; Kortan, R.; Muller, A. J.; Thayer, A. M.; Duncan, T. M.; Douglass, D. C.; Brus, L. *J. Am. Chem. Soc.* **1988**, *110*, 3046–3050.

(10) Dameron, C. T.; Reese, R. N.; Mehra, R. K.; Kortan, A. R.; Carroll, P. J.; Steigerwald, M. L.; Brus, L. E.; Winge, D. R. *Nature* **1989**, *338*, 596–7.
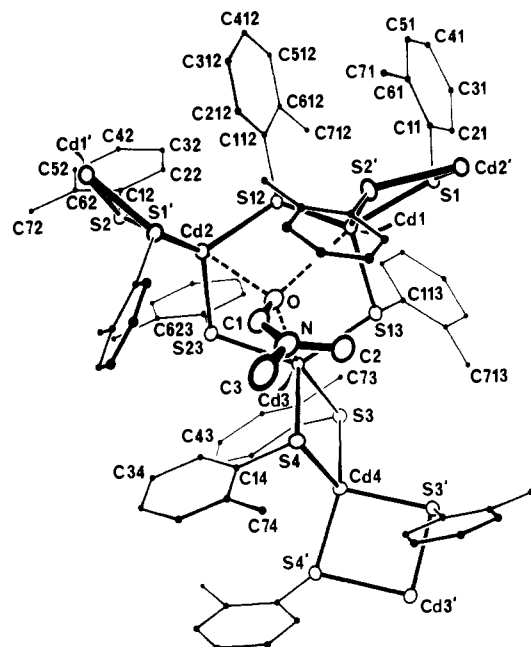
Figure 1. Local coordination structure of **5**, with hydrogen atoms omitted for clarity. Atoms with unprimed labels define the asymmetric unit: the sequence of labeling of carbon atoms around the ring on S*m* is C1*m*, C2*m*, ..., C6*m*, C7*m*, the latter being the methyl carbon atom. A 2_1 axis relates the Cd1, S1, S2, and Cd2 atoms and their primed counterparts at the top of the figure, and a 2-fold axis passes through Cd4. There are connections to the remainder of the lattice through Cd1′, Cd2′, and Cd3′. The minor disorder component of the S2 ligand is not shown. Cd, S, and DMF atoms are drawn as the 11.5% probability ellipsoids.

Table I. Details of the Crystallographic Analysis for **5**

formula, fw	$Cd_{3.5}S_7C_{49}H_{49}\cdot C_3H_7NO$, 1328.8
space group	$P4_32_12$
a and *b*, Å	14.028 (1)
c, Å	55.295 (8)
V, Å³	10 881 (2)
T, °C	21 (1)
Z	8
D_{calc}, g cm⁻³	1.62
μ, cm⁻¹	16.42
$R = \sum^m |\Delta F|/\sum^m |F_o|$	0.034
$R_w = [\sum^m w |\Delta F|^2/\sum^m w |F_o|^2]^{1/2}$	0.049
transm coeff: max, min	0.78, 0.70

Crystalline **4** is two-dimensionally nonmolecular, again with vertex-linked adamantanoid cages, but with one of the eight Cd atoms in the asymmetric unit coordinated as $(\mu\text{-SAr})_3Cd(DMF)_3$. By employment of ^{113}Cd and ^{13}C NMR spectroscopy, we have shown that in DMF solution, 1–4 exist as macromolecules that most probably contain vertex-linked adamantanoid cages.[11] Under conditions of plasma desorption, rich mass spectra of positive and negative ions can be obtained from compounds Cd(SAr)₂, with extended series of ions $Cd_xS_y(SAr)_z$, with $x \le 9$ and $y \le 7$, and with sequences corresponding to SAr₂ loss.[12,13]

Variation of the substituent in the 4-position in Cd(SAr)₂ compounds has, surprisingly, a pronounced effect on the crystal structure, with three quite different crystal structures among the four compounds 1–4. This 4-substitution does not markedly affect the solution NMR or the PD mass spectra. In this paper we report a new crystal structure of the first compound with a substituent in the 2-position, namely $Cd(SC_6H_4CH_3\text{-}2)_2$ (**5**), as crystallized from DMF.

(11) Dance, I. G.; Garbutt, R. G.; Bailey, T. D. *Inorg. Chem.* **1990**, *29*, 603.
(12) Craig, A. G.; Kamensky, I.; Garbutt, R. G.; Dance, I. G.; Derrick, P. J. *Int. J. Mass Spectrom. Ion Processes* **1988**, *86*, 273.
(13) Craig, A. G.; Kamensky, I.; Garbutt, R. G.; Dance, I. G.; Derrick, P. J. In preparation.

Table II. Fractional Coordinates for the Non-Hydrogen Atoms of **5**

atom[a]	x/a	y/b	z/c
Cd1	0.48687 (4)	0.76099 (4)	0.13882 (1)
Cd2	0.76907 (4)	0.72209 (4)	0.15192 (1)
Cd3	0.58335 (4)	0.64753 (4)	0.20399 (1)
Cd4	0.49245 (4)	0.50755 (4)	0.24999 (0)
S1	0.3412 (1)	0.8775 (1)	0.1322 (0)
S2	0.9364 (2)	0.8003 (2)	0.1517 (1)
S3	0.5148 (1)	0.6880 (1)	0.2466 (0)
S4	0.5624 (2)	0.4618 (1)	0.2095 (0)
S12	0.6408 (1)	0.8465 (1)	0.1462 (0)
S13	0.4379 (1)	0.7054 (1)	0.1810 (0)
S23	0.7549 (1)	0.6846 (2)	0.1969 (0)
S2*	0.9077 (7)	0.8560 (7)	0.1398 (2)
C11	0.3625 (3)	0.9985 (4)	0.1263 (1)
C21	0.3317 (4)	1.0614 (6)	0.1442 (2)
C31	0.3449 (6)	1.1594 (5)	0.1414 (2)
C41	0.3890 (6)	1.1946 (4)	0.1205 (2)
C51	0.4198 (5)	1.1316 (5)	0.1026 (2)
C61	0.4065 (4)	1.0336 (5)	0.1055 (1)
C71	0.4401 (6)	0.9688 (7)	0.0861 (2)
C12	0.9544 (4)	0.9159 (4)	0.1630 (1)
C22	0.8793 (4)	0.9812 (5)	0.1636 (1)
C32	0.8943 (5)	1.0730 (5)	0.1726 (2)
C42	0.9843 (6)	1.0995 (4)	0.1811 (1)
C52	1.0593 (5)	1.0341 (5)	0.1805 (1)
C62	1.0444 (4)	0.9424 (4)	0.1715 (1)
C72	1.1256 (5)	0.8748 (7)	0.1711 (2)
C13	0.6123 (3)	0.7234 (3)	0.2642 (1)
C23	0.6860 (4)	0.6596 (4)	0.2694 (1)
C33	0.7633 (4)	0.6889 (6)	0.2834 (1)
C43	0.7670 (4)	0.7820 (6)	0.2923 (1)
C53	0.6934 (5)	0.8458 (4)	0.2872 (1)
C63	0.6160 (4)	0.8165 (3)	0.2731 (1)
C73	0.5391 (6)	0.8860 (5)	0.2680 (2)
C14	0.6725 (4)	0.4036 (4)	0.2155 (1)
C24	0.7515 (5)	0.4563 (4)	0.2231 (1)
C34	0.8378 (4)	0.4103 (6)	0.2278 (1)
C44	0.8452 (4)	0.3117 (6)	0.2249 (1)
C54	0.7661 (5)	0.2591 (4)	0.2173 (1)
C64	0.6797 (5)	0.3050 (4)	0.2127 (1)
C74	0.5972 (7)	0.2470 (6)	0.2047 (2)
C112	0.6733 (2)	0.9319 (3)	0.1241 (1)
C212	0.7158 (3)	0.9024 (3)	0.1026 (1)
C312	0.7416 (4)	0.9696 (4)	0.0851 (1)
C412	0.7248 (3)	1.0664 (4)	0.0893 (1)
C512	0.6822 (4)	1.0959 (3)	0.1108 (1)
C612	0.6565 (3)	1.0286 (3)	0.1283 (1)
C712	0.6115 (5)	1.0624 (4)	0.1510 (1)
C113	0.4023 (3)	0.8096 (3)	0.1968 (1)
C213	0.4541 (3)	0.8937 (3)	0.1938 (1)
C313	0.4267 (4)	0.9762 (3)	0.2061 (1)
C413	0.3475 (4)	0.9745 (3)	0.2214 (1)
C513	0.2957 (3)	0.8903 (4)	0.2244 (1)
C613	0.3231 (3)	0.8079 (3)	0.2121 (1)
C713	0.2665 (4)	0.7197 (4)	0.2156 (1)
C123	0.7858 (4)	0.7935 (4)	0.2111 (1)
C223	0.7172 (4)	0.8649 (5)	0.2138 (1)
C323	0.7411 (7)	0.9508 (5)	0.2250 (1)
C423	0.8336 (7)	0.9654 (4)	0.2335 (1)
C523	0.9021 (5)	0.8940 (6)	0.2309 (1)
C623	0.8783 (4)	0.8081 (5)	0.2197 (1)
C723	0.9528 (5)	0.7337 (7)	0.2172 (1)
C12*	0.9838 (13)	0.9120 (12)	0.1599 (2)
C22*	1.0743 (15)	0.8716 (16)	0.1621 (4)
C32*	1.1402 (14)	0.9109 (22)	0.1782 (5)
C42*	1.1156 (18)	0.9905 (22)	0.1921 (4)
C52*	1.0250 (20)	1.0308 (17)	0.1898 (4)
C62*	0.9592 (14)	0.9916 (14)	0.1737 (3)
C72*	0.8637 (18)	1.0362 (22)	0.1717 (7)
O	0.6159 (5)	0.6035 (4)	0.1518 (1)
N	0.5697 (6)	0.4512 (5)	0.1438 (2)
C1	0.6335 (8)	0.5218 (7)	0.1467 (2)
C2	0.4644 (9)	0.4667 (8)	0.1477 (3)
C3	0.5991 (11)	0.3532 (8)	0.1382 (3)

[a] Asterisks indicate atoms of the disorder component of the SAr ligand 2.

Table III. Bond Distances (Å) and Angles (deg)[a]

Cd1–S12	2.504 (2)	Cd1–S1	2.642 (2)
Cd1–S13	2.554 (2)	Cd1–S2[b]	2.504 (3)
Cd2–S12	2.526 (2)	Cd2–S2	2.591 (3)
Cd2–S23	2.548 (2)	Cd2–S1[c]	2.556 (2)
Cd3–S13	2.536 (2)	Cd3–S3	2.607 (2)
Cd3–S23	2.493 (2)	Cd3–S4	2.640 (2)
Cd1–O	2.945 (6)	Cd4–S3	2.557 (2)
Cd2–O	2.717 (6)	Cd4–S4	2.526 (2)
Cd3–O	2.988 (6)		
		Cd1–S2*[b]	2.536 (9)
		Cd2–S2*	2.785 (9)
S1–C11	1.755 (6)	S2–C12	1.756 (5)
S3–C13	1.752 (5)	S4–C14	1.777 (5)
S12–C112	1.771 (4)	S13–C113	1.773 (4)
S23–C123	1.773 (6)	S2*–C12*	1.728 (16)
O–C1	1.206 (10)	N–C1	1.345 (12)
N–C2	1.510 (14)	N–C3	1.468 (13)
S12–Cd1–S13	103.2 (1)	S1–Cd1–S2[b]	82.5 (1)
S12–Cd2–S23	102.0 (1)	S2–Cd2–S1[c]	82.5 (1)
S13–Cd3–S23	129.1 (1)	S3–Cd3–S4	94.0 (1)
Cd1–S12–Cd2	107.7 (1)		
Cd2–S23–Cd3	105.8 (1)		
Cd1–S13–Cd3	109.8 (1)		
S1–Cd1–S12	113.2 (1)	S1–Cd1–S13	96.2 (1)
S12–Cd1–S2[b]	123.7 (1)	S13–Cd1–S2[b]	129.6 (1)
S12–Cd2–S1[c]	124.6 (1)	S23–Cd2–S1[c]	129.7 (1)
S2–Cd2–S12	110.6 (1)	S2–Cd2–S23	99.3 (1)
S3–Cd3–S13	95.0 (1)	S3–Cd3–S23	116.9 (1)
S4–Cd3–S13	106.5 (1)	S4–Cd3–S23	109.4 (1)
S3–Cd4–S4	98.0 (1)	S3–Cd4–S3[d]	104.4 (1)
S3–Cd4–S4[d]	114.7 (1)	Cd2–S2*–Cd1[c]	91.1 (3)
Cd1–S1–Cd2[b]	94.0 (1)	Cd2–S2–Cd1[c]	96.6 (1)
Cd3–S4–Cd4	84.0 (1)	Cd3–S3–Cd4	84.0 (1)
O–Cd1–S2[b]	97.7 (1)	O–Cd2–S1[c]	88.6 (1)
S13–Cd1–O	73.4 (1)	S12–Cd2–O	81.9 (1)
S12–Cd1–O	77.8 (1)	S23–Cd2–O	79.3 (1)
S1–Cd1–O	166.7 (1)	S2–Cd2–O	167.3 (1)
S4–Cd3–O	85.7 (1)		
S13–Cd3–O	72.9 (1)		
S23–Cd3–O	75.1 (1)		
S3–Cd3–O	167.1 (1)		
Cd1–O–C1	141.4 (8)		
Cd2–O–C1	114.9 (7)		
Cd3–O–C1	117.0 (7)		
O–C1–N	126.3 (10)	C1–N–C2	121.9 (8)
C1–N–C3	121.9 (9)	C2–N–C3	116.1 (9)

[a] Asterisks indicate atoms of the disorder component of the SAr ligand 2. [b] Symmetry-related atom: −0.5 + *x*, 1.5 − *y*, 0.25 − *z*. [c] Symmetry-related atom: 0.5 + *x*, 1.5 − *y*, 0.25 − *z*. [d] Symmetry-related atom: 1 − *y*, 1 − *x*, 0.5 − *z*.

Table IV. Angles ϕ and θ (deg) at the Doubly Bridging Thiolate Ligands[a]

ligand	θ	ϕ	ligand	θ	ϕ
S1	94.0 (1)	45.7 (3)	S12	107.7 (1)	47.0 (2)
S2	96.6 (1)	33.0 (2)	S13	109.8 (1)	63.2 (2)
S3	84.0 (1)	65.5 (2)	S23	105.8 (1)	60.8 (2)
S4	84.0 (1)	63.0 (2)			

[a] ϕ is the acute angle between the S–C vector and the Cd–S–Cd plane; θ is the Cd–S–Cd angle.

Experimental Section

Preparation and Crystallization. $Cd_7(SC_6H_4CH_3\text{-}2)_{14}(DMF)_2$ (5). A solution of $Cd(NO_3)_2\cdot 4H_2O$ (8.6 g) in methanol (50 mL) was added to a mixture of triethylamine (5.6 g) and 2-methylbenzenethiol (6.9 g) in methanol (50 mL) at 0 °C, in the absence of dioxygen. After the slurry was stirred for 1 h, the precipitate was filtered out, washed well with large volumes of methanol and acetone, and vacuum-dried. The yield was almost quantitative. Crystals were grown by carefully layering a solution in DMF (0.2 g/mL) with ethanol.

Crystallography. An Enraf-Nonius CAD4 diffractometer with monochromatized Mo Kα radiation was used to record intensity data.
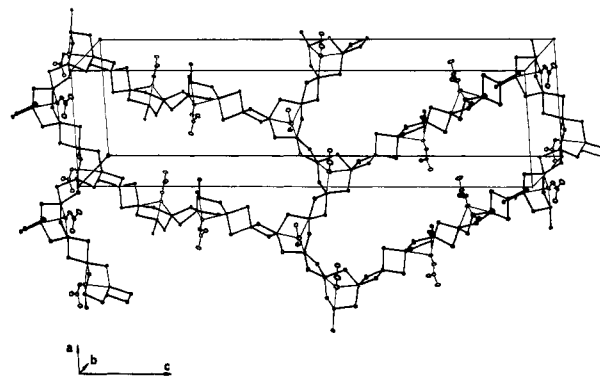
Figure 2. Simplified representation of part of the crystal lattice of **5**. Only Cd, S, and DMF (non-hydrogen) atoms are included. Two of the Cd_{24} macrocycles approximately parallel to the *ac* plane are emphasized by the atoms drawn; corresponding macrocycles approximately parallel to the *bc* plane and displaced from those shown by *c*/4 have been omitted for clarity.

In order to facilitate data collection with such a large cell parameter (*c* = 55.30 Å), the scintillation counter was placed on an extension arm of the diffractometer, which increased the crystal to aperture distance from 173 to 368 mm. The procedures for data collection and reduction and corrections for absorption have been described.[14] Corrections were made for slight decomposition during data collection. Table I contains numerical details of the crystallographic analysis and the final least-squares refinement. Solution of the structure, employing direct methods (MULTAN) and successive Fourier syntheses, yielded the positions of all 65 non-hydrogen atoms. Least-squares refinement used the program RAELS,[15] which allows for rigid-body group refinement. The $C_6H_4CH_3$ sections of the ligands were modeled as rigid groups, with the ring having C_{2v} symmetry and the methyl carbon atom held in the plane of the ring. The ring hydrogen atoms were included as part of the rigid group, while the methyl hydrogen atoms were refined, but slack-constrained to sensible geometry. Each ligand group was refined with TL thermal motion(where T is the translation tensor and L the libration tensor) described by 12 parameters and with the origin fixed on the appropriate S atom. The atoms of the DMF group were refined individually with thermal motion described as TL with the origin on the O atom. The Cd and S atoms were refined anisotropically in the normal way. Refinement converged with *R* = 0.052, but a difference map revealed the presence of a disordered ligand at S2. The second disorder component was therefore included (except the methyl H atoms) with refinement of the proportion of the two components. At convergence, with *R* = 0.036, structure factors were calculated in the alternate space group $P4_32_12$, for which *R* = 0.034. Refinement was therefore completed in this space group to a final residual of 0.034. The refined occupancies for the two disorder components of the ligand at S2 were 0.787 (3) and 0.213 (3): atoms from the lesser component are labeled with an asterisk. The largest peaks in the final difference map were up to 0.8 e Å^{-3}. Several of these peaks could be construed as a small disorder component associated with the ligand on S1, but this disorder was not included in the refinement. Scattering factors, including real and imaginary components of anomalous scattering for Cd and S, were from ref 16. The atom labeling and the asymmetric unit are shown in Figure 1. Coordinates for non-hydrogen atoms are contained in Table II. Additional parameters have been deposited.[17]

Results

Description of the Structure. There are no adamantanoid cages in the structure. Instead there are two fundamental structural units that are connected and linked in a large and three-dimensionally nonmolecular filigree, in an elongated tetragonal unit cell. Our description of the structure begins with the building units and the local cadmium coordination, as shown in Figure 1. Cadmium atoms Cd1, Cd2, and Cd3 and the thiolate ligands S13,

(14) Herath Banda, R. M.; Dance, I. G.; Bailey, T. D.; Craig, D. C.; Scudder, M. L. *Inorg. Chem.* **1989**, *28*, 1862.

(15) Rae, A. D. RAELS: A Comprehensive Constrained Least-Squares Refinement Program. University of New South Wales, 1984.

(16) Ibers, J. A.; Hamilton, W. C., Eds. *International Tables for X-Ray Crystallography*; Kynoch Press: Birmingham, England, 1974; Vol. 4, Tables 2.2A and 2.3.1.

(17) See paragraph at end of paper regarding supplementary material.
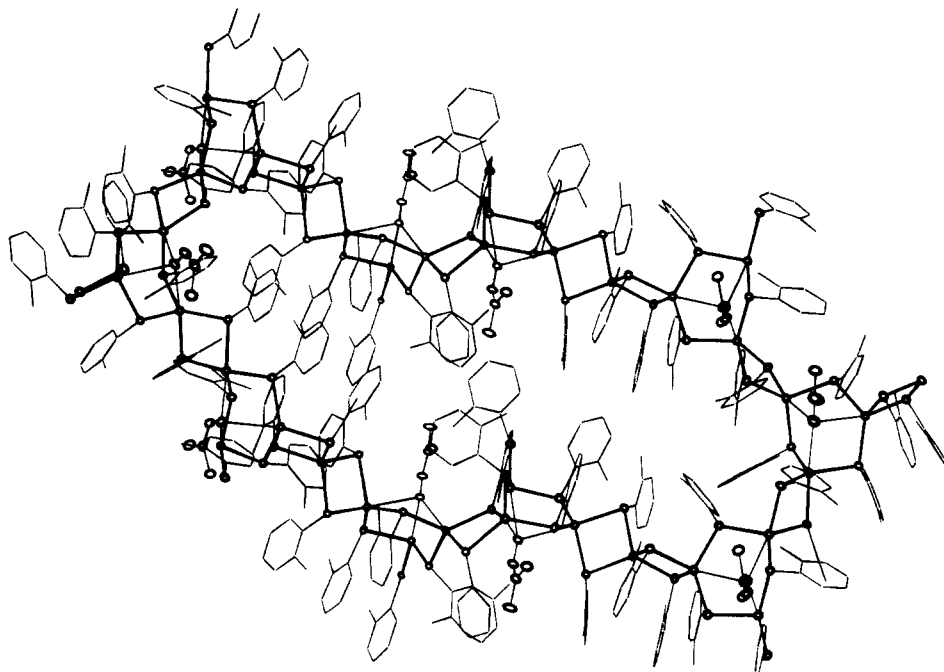
Figure 3. All non-hydrogen atoms associated with one macrocycle in **5**.

S23, and S12 form a $Cd_3(\mu\text{-SAr})_3$ cycle, in chair conformation. The carbonyl oxygen atom (O) of the DMF molecule is weakly coordinated to all three of these cadmium atoms, completing what we denote as the $Cd_3(\mu\text{-SAr})_3(DMF)$, or Cd_3, cycle. Each of the cadmium atoms in this cycle is connected externally through a pair of doubly bridging thiolate ligands to another cadmium atom. In two cases this connection is to another $Cd_3(\mu\text{-SAr})_3(DMF)$ cycle: Cd1 is connected to Cd2 of another cycle, and vice versa, through ligands at S1 and S2. The Cd1(S1)(S2)Cd2 cycle is denoted the Cd_2 cycle. Thus each Cd_3 cycle is connected to two Cd_2 cycles, and vice versa. Cd3 is connected through doubly bridging ligands S3 and S4 to a unique cadmium atom, Cd4, that is tetrahedrally coordinated and located on a 2-fold axis: Cd4 provides a spiro connection to another $Cd_3(\mu\text{-SAr})_3(DMF)$ cycle. The Cd3(S3)(S4)Cd4 cycle is labeled the *spiro*-Cd_2 cycle. Thus the asymmetric unit has the composition $(\mu\text{-SAr})_3Cd_3(DMF)$-$(\mu\text{-SAr})_2(\mu\text{-SAr})_2Cd_{0.5}$.

Local and Coodination Geometry. Bond distances and angles are presented in Table III. The Cd–O distances of 2.72, 2.95, and 2.99 Å are very long and indicative of weak interactions. They are in stark contrast to the Cd–O(DMF) distances of 2.28, 2.31, and 2.45 Å at the $Cd(\mu\text{-SAr})_3(DMF)_3$ coordination site in **4**. We consider it significant that in **5** the three Cd–O distances are unequal and that it is the Cd–O linkage (Cd2–O) trans in the Cd–O–C–N coordination that is substantially shorter. This is consistent with the recently recognized stereochemical differentiation of the bonding strengths of the anti and syn lone pairs at carbonyl oxygen atoms.[18] Apart from these weak interactions with DMF, all cadmium coordination is essentially tetrahedral $Cd(\mu\text{-SAr})_4$, necessarily distorted at the connection to the Cd_2 cycles and slightly distorted also by the asymmetry of substituent configuration in the Cd_3 cycle.

The Cd_3 cycle has distorted-chair conformation: the deviations of the S atoms from the Cd_3 plane are 1.38 Å (S12), 0.14 Å (S13), and 0.46 Å (S23), while the torsional angles around the cycle are −85.7° (at S12–Cd2), 51.9° (at Cd2–S23), −27.4° (at S23–Cd3), 21.2° (at Cd3–S13), −40.2° (at S13–Cd1), and 77.4° (at Cd1–S12). As is apparent from Figure 1, the ligand substituents at S13 and S23 are axial to the Cd_3 cycle: the consequence of the substituent repulsion this incurs is a substantial opening of the S13–Cd3–S23 angle to 129.1°, in contrast to the corresponding intracycle angles of 103 and 102° at Cd1 and Cd2. The intracycle

angles at S12, S23, and S13 are not affected. These geometrical influences of axial aryl substituents are well-known.[19]

In the Cd_2 cycle that connects Cd_3 cycles, the angles at Cd are 7.5° less than 90°, while those at S are 94 and 97°. The angle of folding of the cycle at the S- - -S hinge is 21.1°, and the ligand substituents are trans relative to the S- - -S vector. It can be seen in Figure 1 that the aromatic ring on S2 is parallel to the plane of the DMF molecule, but there are no anomalous contacts. A minor proportion (21%) of the ligand at S2 occurs at an alternative disordered location (S2*, not shown in the figures), corresponding to inversion of the fold of the Cd_2 cycle and inversion of the pyramidal configuration at S2.

Distances and angles around the spiro Cd4 atom and in the spiro Cd_2 cycles are normal. The substituents at S3 and S4 are cis relative to the S3- - -S4 vector, and the cycle is folded only by 2.4° at the S3- - -S4 hinge. There is a wider range of Cd–S distances in this structure than in the $Cd(SAr)_2$ structures containing adamantanoid cages.

As in other structures with doubly bridging thiolate ligands, we have assessed the stereochemistry at the pyramidal S atom in terms of the (acute) angle ϕ between the S–C vector and the Cd–S–Cd plane[19] and noted little correlation with the Cd–S–Cd angle. These values are given in Table IV.

Lattice Structure. The lattice structure of this compound is unique. In general terms, the lattice is three-dimensionally nonmolecular, with each Cd_3 cycle linked to three others and chains of these connections occurring along all three of the crystal axial directions. The chains are propagated by the axial 4_3 screw axes and the lateral 2_1 screw axes of the tetragonal space group $P4_32_12$, and the lateral 2-fold axes pass through the spiro Cd atom. However the unit cell is very long, 55.3 Å, with $a = b = 14.0$ Å, and it is easier and more informative to describe the structure, not in terms of the symmetry operations applied to the asymmetric unit, but in terms of the very large cycles (hereafter denoted as the macrocycles) that exist in this crystal. The macrocycles that are approximately parallel to the ac plane are shown in Figure 2. The macrocycle is unfolded and elongated, being ~28 Å ($c/2$) long and 14 Å (a, b) across. Around each macrocycle there are ten Cd_3 cycles, six Cd_2 cycles, and four spiro Cd atoms. Each end of the macrocycle comprises the sequence of cycles[20] {Cd_3–Cd_2–Cd_3–Cd_2–Cd_3} (propagated by a 2_1 screw axis), while along the long edges of the macrocycle the sequence of units is {*spiro*-

(18) Marshall, L.; Parris, K.; Rebek, J.; Luis, S. V.; Burguete, M. I. *J. Am. Chem. Soc.* **1988**, *110*, 5192 and references cited therein.

(19) Dance, I. G. *Polyhedron* **1986**, *5*, 1037.

(20) In this representation Cd atoms are shared between contiguous cycles.
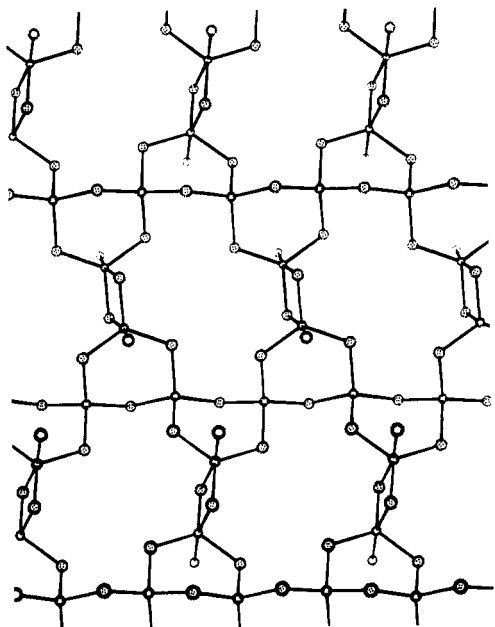
Figure 4. Two-dimensionally nonmolecular pattern of Cd (small open circles) and S (stipled circles) atoms in crystalline $^2_\infty\{Cd(SCH_2CH_2OH)_2\}$ (6). The open circles linked to Cd represent coordinated alcohol functions.

Cd_2-*spiro*-Cd_2-Cd_3-Cd_2-Cd_3-*spiro*-Cd_2-*spiro*-$Cd_2\}$. Around the macrocycle, the pathway with the smallest number of connections involves 24 cadmium atoms bridged by 24 thiolate ligands (each Cd_3 cycle contributes one thiolate bridge in this pathway).

The macrocycles form a pseudoherringbone pattern, shown in two dimensions in Figure 2, but which is actually three-dimensional as a consequence of the tetragonal symmetry of the lattice and the 4-fold screw axes parallel to *c*. The Cd_3 cycles on the edges of the macrocycle provide the linkages to other macrocycles that are approximately perpendicular to those shown in Figure 2 and are translated by *c*/4. Thus each macrocycle is externally connected to other macrocycles at ten points, generating a rather complex three-dimensional network. It is possible to describe this structure in different ways and to trace connections and chains of the small cycles other than those emphasized by the macrocycles in Figure 2.

Figure 3 shows the ligand 2-methylphenyl groups associated with one macrocycle. The major feature to notice is that the aryl groups are directed away from the chain and away from the DMF ligands.

Discussion

The DMF molecule tripodally located over the face of the Cd_3 cycle is an unusual but rationalizable feature. All Ar substituents on a $Cd_3(\mu\text{-}SAr)_3$ cycle, whether axial or equatorial, must be located on one side of the plane of the cycle, leaving the opposite face vacant. Because the Ar substituents on the adjoining Cd_2 cycles cannot intrude over this vacant face, there is space for a small molecule such as DMF.

The crystal structure of **5** contains features similar to those in the crystal structure of the cadmium alkanethiolate $^2_\infty\{Cd(SCH_2CH_2OH)_2\}$ (6),[21] which is outlined in Figure 4. There exist in **6** $Cd_3(\mu\text{-}SR)_3$ cycles and $Cd_2(\mu\text{-}SR)_2$ cycles, spiro-linked at cadmium, as in **5**, but in **6** they occur in a two- rather than a three-dimensionally nonmolecular network. Some of the ligand hydroxy functions in **6** provide secondary coordination at one of the two types of Cd atoms, while there is extensive intra- and interlayer hydrogen bonding of the ligands. In **6**, the proportion of the crystal volume occupied by the ligands is smaller than in the $Cd(SAr)_2$ compounds.

Why are there no adamantanoid cages in the crystal structure of **5**? We presume that the 2-methyl substituent on the ligand aryl group causes steric interference. Although the adamantanoid cage is paradigmatic in molecular cadmium arenethiolate compounds,[22-25] it has not yet been confirmed for any arenethiolate ligand with a substituent in the 2-position, and it is now well established that bulkier 2-aryl substitution disrupts molecular structures of metal thiolates even further.[26-28] Our preliminary results on the [113]Cd NMR spectra of **5** in DMF solution show appreciable differences from the behavior of **1–4**.

Supplementary Material Available: Table S1, listing atomic coordinates, thermal parameters, and distances and angles for **5**, and Table S2, giving crystallographic details pertaining to data collection, processing, and refinement of the structures of **5** (10 pages); a listing of structure factors for **5** (19 pages). Ordering information is given on any current masthead page.

(21) Burgi, H. B. *Helv. Chim. Acta* **1974**, *57*, 513.
(22) Hagen, K. S.; Stephan, D. W.; Holm, R. H. *Inorg. Chem.* **1982**, *21*, 3928.
(23) Hagen, K. S.; Holm, R. H. *Inorg. Chem.* **1983**, *22*, 3171.
(24) Dean, P. A. W.; Vittal, J. J. *Inorg. Chem.* **1986**, *25*, 514.
(25) Dean, P. A. W.; Vittal, J. J.; Payne, N. C. *Inorg. Chem.* **1987**, *26*, 1683.
(26) Koch, S. A.; Millar, M. *J. Am. Chem. Soc.* **1983**, *105*, 3362.
(27) Koch, S. A.; Fikar, R.; Millar, M.; O'Sullivan, T. *Inorg. Chem.* **1984**, *23*, 122.
(28) Blower, P. J.; Dilworth, J. R. *Coord. Chem. Rev.* **1987**, *76*, 121.

Notes

Contribution from the Department of Chemistry,
University of Colorado at Colorado Springs,
Colorado Springs, Colorado 80933-7150

Synthesis and Characterization of Rhenium(I) Complexes Bound to the Bridging Ligand 2,3-Bis(2-pyridyl)pyrazine

Ronald Ruminski* and R. Thomas Cambron

Our research group has been interested in the design and characterization of mono- and bimetallic low-spin d^6 transition-metal complexes bound through nitrogen aromatic heterocyclic ligands such as 2,3-bis(2-pyridyl)pyrazine (dpp) and 2,3,5,6-tetrakis(2-pyridyl)pyrazine (tppz), for potential use in photon-

capture/excited-state energy-transfer processes.[1] Several studies have recently demonstrated that rhenium carbonyl centers bound with 2,2'-bipyrimidine (bpm) and other pyridyl ligands have highly absorbing MLCT bands in the visible spectrum and are emissive and electrochemically stable, making them ideal fragments in photon-capture energy-transfer processes.[2-7] Thus, a relatively

(1) (a) Ruminski, R. R.; Johnson, J. J. *Inorg. Chem.* **1987**, *26*, 210. (b) Shoup, M.; Hall, B.; Ruminski, R. R. *Inorg. Chem.* **1988**, *27*, 200. (c) Wallace, I.; Ruminski, R. R. *Polyhedron* **1987**, *6*, 1673. (d) Ruminiski, R. R.; Cockroft, T.; Shoup, M. *Inorg. Chem.* **1988**, *27*, 4026. (e) Ruminski, R.; Kiplinger, J.; Cockroft, T.; Chase, C. *Inorg. Chem.* **1989**, *28*, 370.
(2) Sahai, R.; Rillema, D. P.; Shaver, R.; Van Wallendael, S.; Jackman, D. C.; Boldaji, M. *Inorg. Chem.* **1989**, *28*, 1022.
(3) Vogler, A.; Kisslinger, J. *Inorg. Chim. Acta* **1986**, *115*, 193.
(4) Juris, A.; Campagna, S.; Bidd, I.; Lehn, J.-M.; Ziessel, R. *Inorg. Chem.* **1988**, *27*, 4007.